forests

MDPI

Article

The European Heat Wave 2018: The Dendroecological Response of Oak and Spruce in Western Germany

Burkhard Neuwirth [1], Inken Rabbel [2], Jörg Bendix [3], Heye R. Bogena [4] and Boris Thies [3,*]

[1] DeLaWi Tree–Ring Analyses, Preschlinallee 2, 51570 Windeck, Germany; delawi@t-online.de
[2] Department of Geography, University of Bonn, Meckenheimer Allee 166, 53115 Bonn, Germany; irabbel@uni-bonn.de
[3] Laboratory for Climatology and Remote Sensing & Faculty of Geography, University of Marburg, Deutschhausstraße 12, 35037 Marburg, Germany; bendix@staff.uni-marburg.de
[4] Forschungszentrum Jülich GmbH, Agrosphere Institute (IBG-3), 52425 Jülich, Germany; h.bogena@fz-juelich.de
* Correspondence: thies@staff.uni-marburg.de; Tel.: +49-6421-28-25910

Abstract: The European heat wave of 2018 was characterized by extraordinarily dry and hot spring and summer conditions in many central and northern European countries. The average temperatures from June to August 2018 were the second highest since 1881. Accordingly, many plants, especially trees, were pushed to their physiological limits. However, while the drought and heat response of field crops and younger trees have been well investigated in laboratory experiments, little is known regarding the drought and heat response of mature forest trees. In this study, we compared the response of a coniferous and a deciduous tree species, located in western and central–western Germany, to the extreme environmental conditions during the European heat wave of 2018. Combining classic dendroecological techniques (tree–ring analysis) with measurements of the intra–annual stem expansion (dendrometers) and tree water uptake (sap flow sensors), we found contrasting responses of spruce and oak trees. While spruce trees developed a narrow tree ring in 2018 combined with decreasing correlations of daily sap flow and dendrometer parameters to the climatic parameters, oak trees developed a ring with above–average tree–ring width combined with increasing correlations between the daily climatic parameters and the parameters derived from sap flow and the dendrometer sensors. In conclusion, spruce trees reacted to the 2018 heat wave with the early completion of their growth activities, whereas oaks appeared to intensify their activities based on the water content in their tree stems.

Keywords: dendrometer; sap flow; daily correlations; tree–ring width; physiological response

Citation: Neuwirth, B.; Rabbel, I.; Bendix, J.; Bogena, H.R.; Thies, B. The European Heat Wave 2018: The Dendroecological Response of Oak and Spruce in Western Germany. *Forests* **2021**, *12*, 283. https://doi.org/10.3390/f12030283

Received: 8 December 2020
Accepted: 26 February 2021
Published: 2 March 2021

1. Introduction

The summer of 2018 was the second hottest in Germany since 1881 after the hot summer of 2003. This also holds for the federal states of North Rhine–Westphalia (NRW) and Hesse. At the same time, 2018 was characterized by the driest summer conditions in Hesse and the second driest in NRW since 1881 [1]. It was shown by several authors that a specific configurations of the tropospheric Rossby wave circulation (wavenumber–5 and, in 2018, –7 circulation patterns) are responsible for heat waves in Europe and Germany. These configurations were also observed during the previous European and German heat waves of 2003, 2006, and 2015. The occurrence of the wavenumber–7 pattern has particularly increased over recent decades, which is most likely related to climate change effects [2–5].

The consequences of the 2018 heat wave on vegetation were observed by remote sensing over wider areas. The heat summer of 2018 was characterized by the highest negative anomalies in the Leaf Area Index (LAI) over NW–Europe since 2000, particularly in July 2018 [6]. In comparison, Buras et al. [7] found a stronger negative water balance

anomaly for Germany from April to June (AMJ), which led to a clear reduction in vegetation activity measured by vegetation indices (Normalized Difference Vegetation Index—NDVI and Enhanced Vegetation Index—EVI). In addition to these large scale effects, it is of great applied interest for foresters to investigate how common trees species in German forests will react to increasing heat and drought summer conditions. A comparative study for several European tree species revealed that oak was negatively affected by high precipitation in combination with a high N deposition, while beech showed lower growth performances under higher temperatures and drought stress [8].

A comprehensive study for Switzerland revealed that the radial growth of spruce was strongly and enduringly reduced by spring droughts and that this species showed the poorest resistance to droughts among the investigated species. In comparison, broadleaved oak (while sensitive to late frosts) and beech (to a lower extent) showed higher resistance and resilience to spring droughts and are, thus, better adapted to droughts than spruce [9]. By comparing oaks and beeches in European mixed forests, beech was found to be negatively affected by summer droughts, while oak species were negatively affected primarily by spring droughts, beeches showed a fast reaction with growth decreases and recovery (under rain), in comparison to delayed growth reactions for droughts but a longer recovery time for oaks [10].

Our understanding of the effects of extreme climatic events on tree growth are based on the assumption of a decline in net photosynthesis, which is attributed to numerous processes, including increased photorespiration, increased mitochondrial respiration, and the inactivation of Rubisco attributed to a reduced activity of Rubisco activase and so on [11]. After the drought event in 1976, which was one of the strongest drought events in the 20th century [12,13], Hinckley et al. [14] already described the consequences of extreme dry events for eight tree species (including three oak species) in the Ashland Wildlife Area (Missouri/USA) and documented, in particular, a reduced stem growth and depressed net photosynthetic rate to near the compensation point.

They regarded stomatal closure as a drought–avoidance mechanism and that this mechanism represented a trade–off between continued transpiration and photosynthesis [15]. Zweifel et al. [16] underlined in their study of oak, pine, and spruce in the Swiss Valais for the dry event of 2003, the importance of precipitation for the radial growth of all three species, whereby the direct effect of rain on radial growth was most likely caused by a (sudden) release of the pressure conditions in the tree, thus, leading to positive pressure conditions in the cambium [17,18]. Hsiao & Acevedo [17] found two different sensitivities to drought in the growth process: one is related to cell division and the other to cell expansion, the latter being much more sensitive to tree water deficits. Thus, new cells can be formed but not expanded under drought conditions. Only if the drought lasts too long, cell division does stop [16].

The effects of extreme climatic events, in particular drought, on tree stem growth and the associated physiological mechanisms are still not fully understood. On the one hand, they are not only determined by the conditions of previous months [19,20], additionally they are also forced by the conditions of previous years [21–23]. Despite these so–called legacy effects [24], numerous studies have proven the direct effects of the current conditions on stem growth [25–29]. Regardless of the region and/or tree species, these and other similarly focused studies come to the almost uniform conclusion that drought effects have a negative impact on radial growth and lead to a narrow tree ring. Burri et al. [30] stated in their multi–species study on the reactions of Swiss forest trees to the heat of summer 2015, that the effects, however, need a priori to not be negative and explain this with the time of occurrence of the extreme event within the growing season.

The aim of this paper is to compare the response of two tree species in the West German lower mountain ranges in the summer heat of 2018. Therefore, classical dendroclimatological findings from long–term climate–growth relationships and pointer year analyses are combined with temporally high–resolution dendro–physiological analyses (dendrometer and intercellular sap flow) and compared with local climate parameters. In

particular, we test the hypothesis that, as a consequence of the drought, (i) physiological activities were reduced and (ii) a growth reduction occurred ultimately, i.e., a narrow tree ring was formed.

2. Materials and Methods

2.1. Research Sites

The trees examined in this study were from two different research sites in the lower mountain ranges of Western Germany. The spruce site EIFEL (EIF) is located in the Wüstebach catchment in the southwest of the Eifel National Park, North Rhine–Westphalia (a detailed site description for EIF is found in Bogena et al. [31]), while the oak site Universitätswald Marburg (UWM) is located in the Marburg Open Forest (Marburg university forest) [32] near Caldern in the Lahn–Dill mountain country, Hesse. The EIF site is covered by a 70–years–old spruce plantation (*Picea abies* Karst.), which was established after the Second World War at 620 m a.s.l. The soils are characterized by a silty clay loam texture with a medium to high coarse material fraction and a litter layer on top [33]. The UWM site is an over 250–years–old oak (*Quercus petraea* L.) stand, which is located within a mixed beech forest in approx. 270 m a.s.l. This forest has developed on the basis of natural rejuvenation. The dominant soil texture is silt loam [34]. Cambisol is the predominant soil type on both sites. However, the available water capacity (AWC) at the UWM site (~80 mm) is lower than at the EIF site (~250 mm) with an average soil water content for the period 2010–2013 being ~40% for EIF [35]. The two sites slightly vary in aspect and slope (Table 1).

Table 1. Overview of the stand and site characteristics.

Site	Coordinates Long./lat. [°]	Species	Chrono [Year]	MSL [Year]	AGR [mm]	Elev. [m a.s.l.]	Asp. [°]	Slope [%]	Temp. [°C]	Prec. [mm]
EIF	6.331/50.505	PCAB	1958	60	3.78	610	90	10.5	12.5	484
UWM	8.684/50.842	QUPE	1959	155	1.41	270	230	32.5	14.0	77.6

AGR = average growth rate in the period 1960–2018, Asp. = aspect, Chrono = first year of the tree–ring width chronology based upon at least three trees, Elev. = elevation, MSL = mean segment length, PCAB = *Picea abies* (spruce), Prec. = sum of precipitation from March to September 2018, QUPE = *Quercus petraea* (sessile oak), Temp. = mean temperature from March to September 2018.

Both sites are synoptically influenced by atmospheric flows that predominantly originate from the Atlantic Ocean [36]. While the temperature conditions among EIF and UWM are similar, the precipitation varies in both the mean annual precipitation sums and the seasonal precipitation distribution (Figure 1; black lines and grey areas). In the Eifel region, the mean annual precipitation reaches 1280 mm at the German Weather Service (Deutscher Wetterdienst—DWD) weather station Kall–Sistig (located in 9.6 km from the EIF site with a maximum in winter) [37]. Central Hesse, in contrast, is characterized by a mean annual precipitation sum of only 700 mm (DWD weather station Giessen–Wettenberg) with a minimum in February. However, the mean summer precipitation is similar among plots and differs by only 60 mm per month (Figure 1).

In 2018, the temperature showed comparable conditions among the study sites. However, the temperatures in April and July 2018 (red and green lines in Figure 1) exceeded the long–term averages (black lines in Figure 1) by approximately 3 °C. The good fit between the 2018 temperatures recorded by the local weather stations (green lines in Figure 1) and the regional long–term references (red lines in Figure 1) underlines the representativeness of the reference stations for our research sites. The precipitation situation is a bit more complex. The 2018 precipitation at the EIF site roughly corresponds to the 2018 values recorded by the regional weather station Kall–Sistig. Both 2018 records also principally correspond to the regional long–term values.

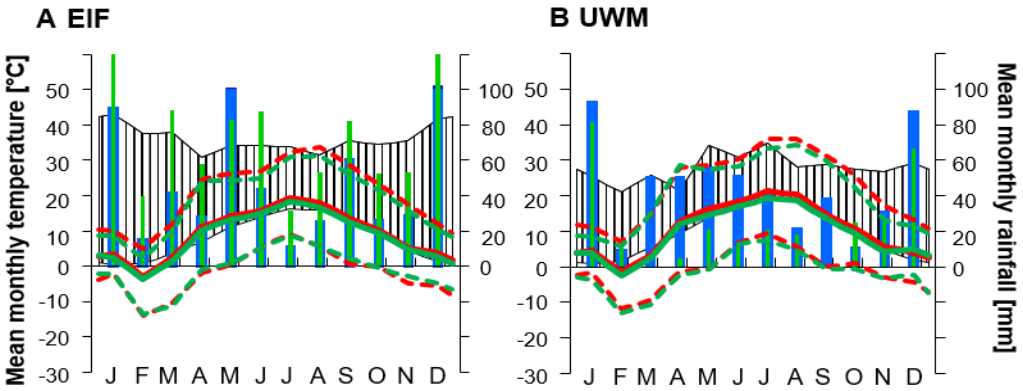

Figure 1. The monthly mean, maximum, and minimum air temperatures (green solid and dashed lines) and monthly precipitation sums (green bares) for 2018 measured at the Eifel (A, EIF) and Marburg university forest (B, UWM) research sites. In addition, data from nearby DWD stations (Kall–Sistig for EIF and Gießen–Wettenberg for UWM) is presented for comparison. For 2018, the temperature and precipitation data is presented as red lines and blue bars, while the long–term data (1981–2010) is presented with the mean monthly precipitation (upper black lines), mean monthly temperatures (lower black lines), and months with humid conditions (black striped areas).

In July and August, the precipitation was significantly lower in 2018 than for the long–term (50 instead of 80 mm; blue and green bars in Figure 1A). At the UWM site, in contrast, we observed a very pronounced precipitation deficit in 2018 (Table 2). The precipitation deficit on site (green bars in Figure 1B) was even well below that recorded by the Giessen–Wettenberg reference station (blue bars in Figure 1B). The deficit started already in February (20 instead of 80 mm precipitation) and continued undiminished until late autumn. During the entire vegetation period, only 10% of the long–term precipitation sum was reached at the UWM site.

Table 2. Comparison of the mean temperatures and precipitation totals in both research sites for various time periods and climate stations.

	EIF			UWM		
Time Period	**Temp. Annual Mean [°C]**	**Prec. Annual Sum [mm]**	**Prec. Seasonal * Sum [mm]**	**Temp. Annual Mean [°C]**	**Prec. Annual Sum [mm]**	**Prec. Seasonal * Sum [mm]**
1981–2010	8.0	859	468	9.6	666	462
2018 DWD–Station	9.5	589	298	10.9	540	319
2018 Local station	8.5	1003	448	9.8	287	102

* The seasonal precipitation sum corresponds to the growing season (here from April to October).

2.2. Dendroecological Observations

To evaluate the long–term climate–growth response of the two research sites, we used annually resolved tree–ring data. The short–term eco–physiological response during the heat year 2018 was monitored using sap flow measurements and dendrometers.

The tree–ring data were collected from 15 trees per research site. From each tree, we extracted two opposite 5 mm cores at breast height. The tree–ring samples were prepared following standard procedures [38]. Tree–ring widths were measured using a LinTab measurement table [39] with a measuring accuracy of 0.01 mm. After a quality check [40,41], the tree–ring series were averaged to tree mean curves (TMC). We detrended the TMC using a high–pass filter based on 5–year weighted moving averages. Ring widths indices were then calculated as ratio between the actual tree–ring width and the filtered value.

To identify years of extreme growth (pointer years, PY), we also calculated so–called Croppervalues C_y [42] from the TMC. To this end, we determined the ratios of the TMC

and their 13–year moving averages and normalized the resulting data series applying a z–transformation [43]. The thresholds for the pointer year description were defined as follows:

$|C_{yz}| = 1.0$ for a weak, $|C_{yz}| = 1.28$ for a strong, and $|C_{yz}| = 1.645$ for an extreme pointer year. These thresholds correspond to the upper 16%, 10%, and 5% quantiles of the standard normal distribution [44,45].

At each site, 3 of the selected 15 trees were instrumented with sap flow sensors and dendrometers. Both measuring devices were installed at breast height on the northern side of the stem. The data were recorded with a datalogger (type CR1000, Campbell Scientific Ltd., Logan, UT, USA) in 30–minute time steps. The course of these half–hourly data over the measurement period from April 10 to September 15 2018, averaged over the three trees at each site, as well as the range of individual trees around the mean, are shown in the supplements (Figure S1). Following Deslauriers et al. [46,47] the stem radius (SR) changes detected by the dendrometers (Type RD, Ecomatik, Dachau, Germany) were resolved into periods of (1) stem contraction due to water loss (transpiration during the day); (2) reversible stem expansion (refilling of the stem water storage during the night), and (3) irreversible stem increment (DM–SRI) and thus growth.

The sap flow activity of the trees was monitored using Granier–type sap flow sensors (SF–L 20/33, Ecomatik, Dachau, Germany). This measuring system basically consists of two sensor probes that are inserted radially into the sapwood, one above the other. While the upper sensor probe is heated, the lower one measures the reference temperature of the wood. The sap flux density within the xylem is now derived from the temperature difference between two probes. The respective equation follows empirical relations [48,49]:

$$SFD = 119 \cdot \left(\frac{\Delta T_{max} - \Delta T}{\Delta T} \right)^{1.231} \quad (1)$$

where SFD is the sap flux density ($g \cdot m^{-2} \cdot s^{-1}$), ΔT is the actual temperature gradient between the two probes, and ΔT_{max} is the maximum temperature gradient measured between the probes in a given time period. The length of this time period depends on the prevailing environmental conditions, because ΔT_{max} represents a state of zero sap flux. We identified ΔT_{max} using the approach of Oishi et al. [50,51], where the ΔT stability and biophysical conditions (vapor pressure deficit ≤ 0.05 kPa; global radiation < 5.0 $W \cdot m^{-2}$) are used as zero flow indicators [52].

To scale the SFD to the sap flow (SF) per tree, we multiplied the SFD by the sapwood area. The sapwood area was derived from the sapwood depths we recorded directly after coring the trees. Finally, the sap flow data was averaged to site–specific mean curves and aggregated to daily sums (SF–SUM). The courses of the site–specific mean curves are shown with the corresponding spans of the individual trees in the supplements (Figure S2 for UWM and Figure S3 for EIF).

2.3. Climate Data and Statistical Analyses

To investigate the mean climate–growth response of the trees in the period 1960–2018, we used the time series of regional German Weather Service (DWD) stations, because the climate stations installed on site only covered recent years. For the EIF site, we chose the DWD station Kall–Sistig as a long–term reference. This station is located about 15 km east of the EIF site at 505 m a.s.l. For the UWM site, we used the DWD station Giessen–Wettenberg, which is located about 25 km south of the UWM site at 203 m a.s.l. The investigation period was limited by the comparably young age of the EIF spruce site and was set to AD 1960 to 2018. For this period, we calculated the mean monthly temperatures and monthly precipitation sums over a 13–month window, from October of the previous year of ring formation to October of the current year of ring formation.

Additionally, we calculated 11 seasonal values and also the annual temperature means and precipitation sums. This procedure resulted in each 24 time series of temperature means and precipitation sums per research site and, thus, in a total of 96 time series for

both locations. Long–term trends were removed from all 96 time series analogously to the treatment of the annual tree–ring data, where the actual values were divided by their 5–year weighted moving averages (see above). To analyze the high–frequency climate–growth response of the trees, we finally correlated the resulting indexed climate data series with the indexed tree–ring data using Pearson's correlations.

To investigate the eco–physiological response of the trees to the heat wave 2018, we used climate data collected in direct proximity to the investigated trees. At the EIF site, the temperature (T) and relative humidity (RH) were measured in 2 m above the soil surface and, thus, within the stand, whereas the precipitation (PCP) and global radiation (RAD) were recorded by the TERrestrial ENviromental Observatories (TERENO) meteorological tower [53] at 38 m height and, thus, above the forest canopy. At the UWM site, we used the records of the Laboratory for Climatology and Remote Sensing (LCRS) climate stations (50.8405° N/8.6832° E), which measure the temperature and relative humidity at 2 m above ground level within the stand, while the precipitation and global radiation were recorded at about 200 m distance from the trees and, thus, without disturbance by the forest canopy.

For both research sites, the vapor pressure deficit (VPD) was derived from the temperature and relative humidity. For the period from the 1st of April to 15th of September 2018, we calculated the daily averages, daily minima, daily maxima (temperature, relative humidity, and VPD), and daily totals (precipitation) as required. Then, we assigned the days of the 2018 growing season to four groups: wet and dry days in spring (until the 30th of May) and wet and dry days in summer (1st of June onwards). We defined wet days as days with at least 3 mm rainfall. Dry days were defined as when the precipitation sum of the actual day and the 3 days before was less than 3 mm. For each of the selected groups, we calculated the Pearson's correlations between the daily climate parameters and the daily resolved tree data to investigate the eco–physiological response of the trees to synoptic events.

3. Results

3.1. Radial Growth

With 3.8 mm/a, the average growth rate (AGR) of the spruce trees at the EIF site for the period 1960–2018 (grey horizontal line in Figure 2A) was more than 2.5 times higher than the AGR of the oaks at the UWM site (1.4 mm/a; black horizontal line in Figure 2A).

Spruce trees at the EIF site generally had a higher AGR, especially in the early 1960s and after the early 1980s (grey lines in Figure 2A). The wide tree rings in the 1960s can be explained by the age of the spruce trees at the EIF site. During the 1960s, the trees were still in their juvenile phase, where tree rings are typically wider than those of mature trees [54]. The high growth rates during the 1980s were initiated by a thinning event in 1981, which reduced the competition among trees and, thus, improved the growth conditions. The oaks at the UWM site (black lines in Figure 2A), in contrast, were already adult in the 1960s. The thinning activities at UWM, as for example around 2005, were less intensive and therefore only slightly affected the growth on site.

The indexed growth chronologies (Figure 2B) generally show similar growth dynamics among the study sites. Only a few periods, e.g., the years 1983 and 1988 or the first half of the 1990s, are characterized by contrasting growth trends. Respectively, most of the pointer years (years with significant positive or negative growth anomalies; Figure 2C) occurred simultaneously at both sites; however, often with differing intensities. Until 1990, the oaks at UWM showed stronger growth reactions than the spruces at the EIF site (e.g., 1973, 1976, and 1981). This also applies to the year 1976, one of the strongest heat and drought years of the 20th century in the northwestern Central Europe and Britain [55,56], where the spruces at the EIF site "only" developed a stronger negative pointer year ($C_{1976z,EIF} = -1.38$), while the oaks at UWM showed an extreme negative pointer year ($C_{1976z,UWM} = -1.84$). After 1990, this changed, and the growth reaction at the EIF site became stronger than at UWM (e.g., 1995, 2000, 2002, 2006, 2009, and 2011). In only two years, both sites and species showed completely opposite reactions: in 1988, the oaks at UWM revealed an extreme

negative pointer year, while the pointer year at the EIF site was extremely positive. In 2018 (red bars in Figure 2C), the growth reactions at UWM surprisingly was positive, while the spruces at the EIF site showed the expected negative growth reaction with a weak negative pointer value of $C_{2018z,EIF} = -1.1$.

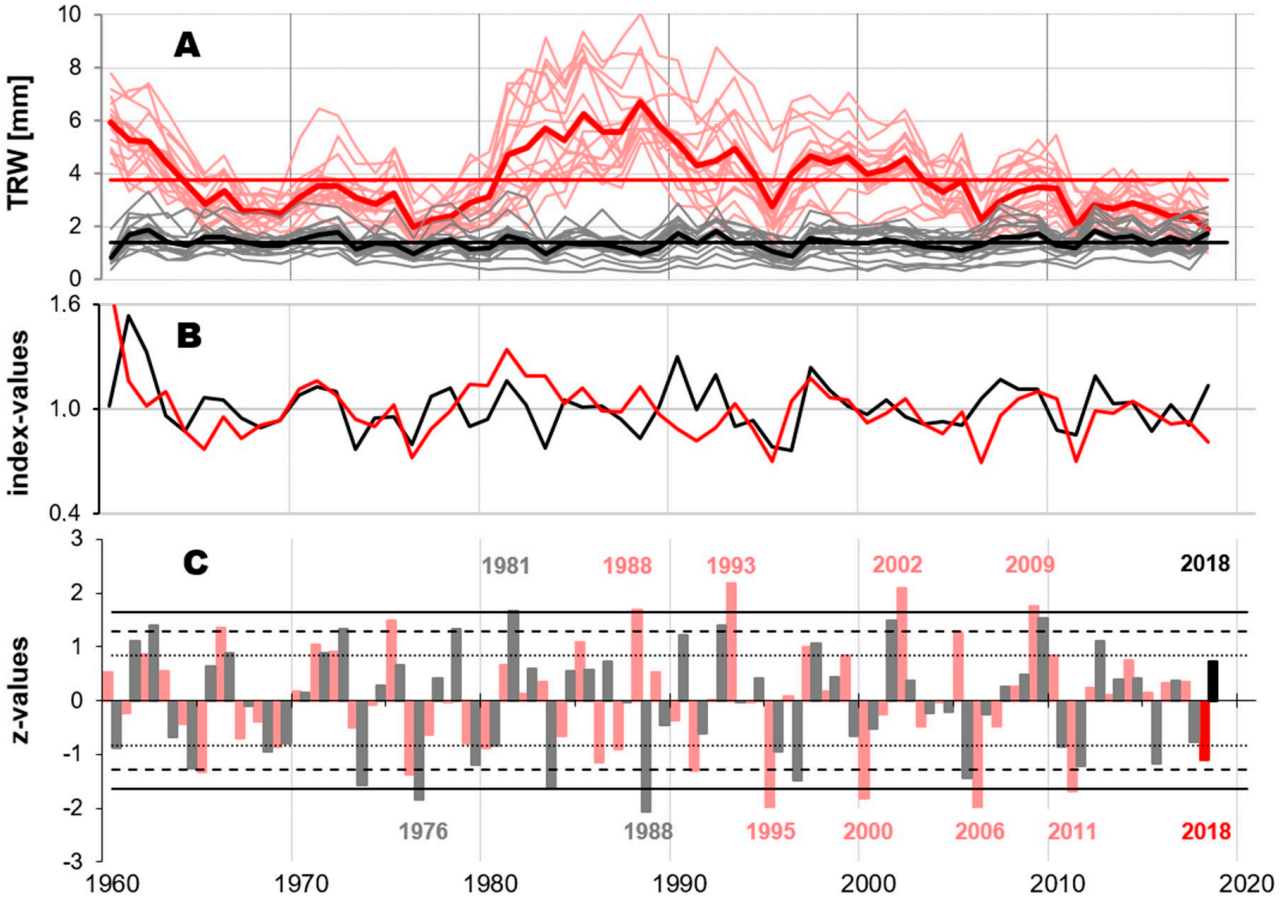

Figure 2. The tree mean curves of 15 trees each for EIF (light red/red) and UWM (grey/black) with corresponding site mean curves (bold lines) and average growth rates (red/black horizontal lines) (**A**), mean indexed tree–ring chronologies (**B**), and z–transformed Croppervalues C_{yz} indicating the so–called pointer years of above–/below–average growth (**C**). The horizontal lines in Part C illustrate the significance levels of the growth anomalies (dotted: $C_{yz} = \pm 0.845$ for weak, broken: $C_{yz} = \pm 1.28$ for strong, and lined: $C_{yz} = \pm 1.645$ for extreme pointer years). Extreme pointer years are marked by years, light red for EIF, grey for UWM, and, for 2018, the bars are highlighted in stronger colors (red and black).

3.2. Interannual Growth/Climate Responses

At the UWM site, the strongest correlation between the tree–ring series and climate data was observed for the June–precipitation ($r_{JUN} = 0.61$; Figure 3A). Further significant positive climate–growth signals were found for precipitation in the extended summer (MJJA) and during the vegetation period (VEG). Hence, water availability was the main growth–limiting factor at the UWM site.

The minor importance of temperature for the oak growth in the region is illustrated by the weak correlations of the mean monthly/seasonal temperatures and the tree–ring data. Only above–average spring temperatures ($r_{MAM} = 0.28$) and below–average summer temperatures ($r_{JJA} = -0.22$) showed positive effects on the tree-ring width (TRW). The spruces at the wetter EIF site, in contrast, predominantly benefited from below–average temperatures during the growing season of the previous year ($r_{JJAv} = -0.42$; Figure 3B). Wet spring conditions ($r_{MAM} = 0.35$) supported spruce growth in the Eifel.

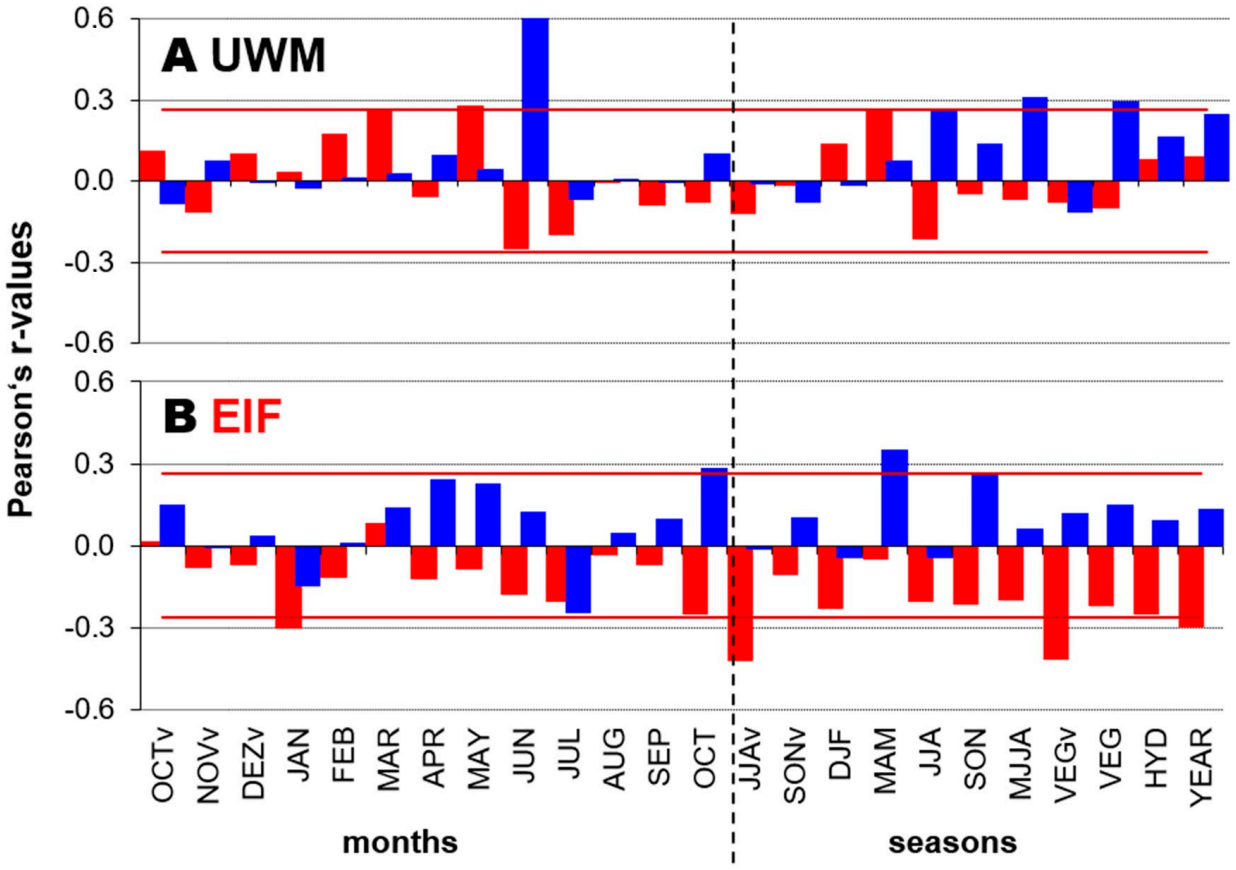

Figure 3. Pearson's correlations between the monthly and seasonal temperature (red bars)/precipitation (blue bars) series and TRW–chronologies for UWM (**A**) and EIF (**B**). Index v designates months and seasons of the previous year of ring formation. Brown horizontal lines mark the level of significance for 95% with r_{krit} = 0.2616.

3.3. Diurnal Sap Flow Activity and Radial Stem Variations in 2018

In spring 2018, both tree species showed typical patterns of physiological activity expressed by inverse diurnal SF and DM cycles (Figure 4A). Following the diurnal dynamics of radiation and vapor pressure deficit, the SF activity rapidly increased before noon, reached the maximum around noon, and decreased toward the late afternoon until reaching near–zero values at night, when the stem water storage was slowly refilled. Only on days with noticeable rainfall, like the 24th of May (Day Of Year—DOY 142), where nearly 10 mm of precipitation was detected at the EIF site, this typical SF pattern is disturbed due to the high relative humidity of the air (low atmospheric demand) and the moist leaf/needle surface. Correspondingly, the DM decreased during the day and increased overnight, when the stem recovered from the water lost during the day. This reversible stem contraction and expansion, which was related to the tree water balance, cell division, and, thus, absolute stem growth, resulted in larger DM maxima from day to day.

In summer 2018 (Figure 4B), the diurnal cycles of DM and SF illustrate the disturbed tree performance after long periods of drought and heat. With 15–18 mL/min, the daily SF maxima were considerably lower than in spring (~20 mL/min). The daily maxima decreased with each dry day. As a consequence, the water absorption in summer (DOY 227–231) was about one–quarter lower than that in spring (DOY 139–143). The stem contraction rates became larger than the expansion rates, which resulted in decreasing DM maxima from day to day, which indicates that the stems were shrinking. On 17th August, a small rainfall event (3 mm) at the EIF site reduced the sap flow activity and allowed for a short recovery of the stem radius. However, this event was too weak to reverse the negative DM trend.

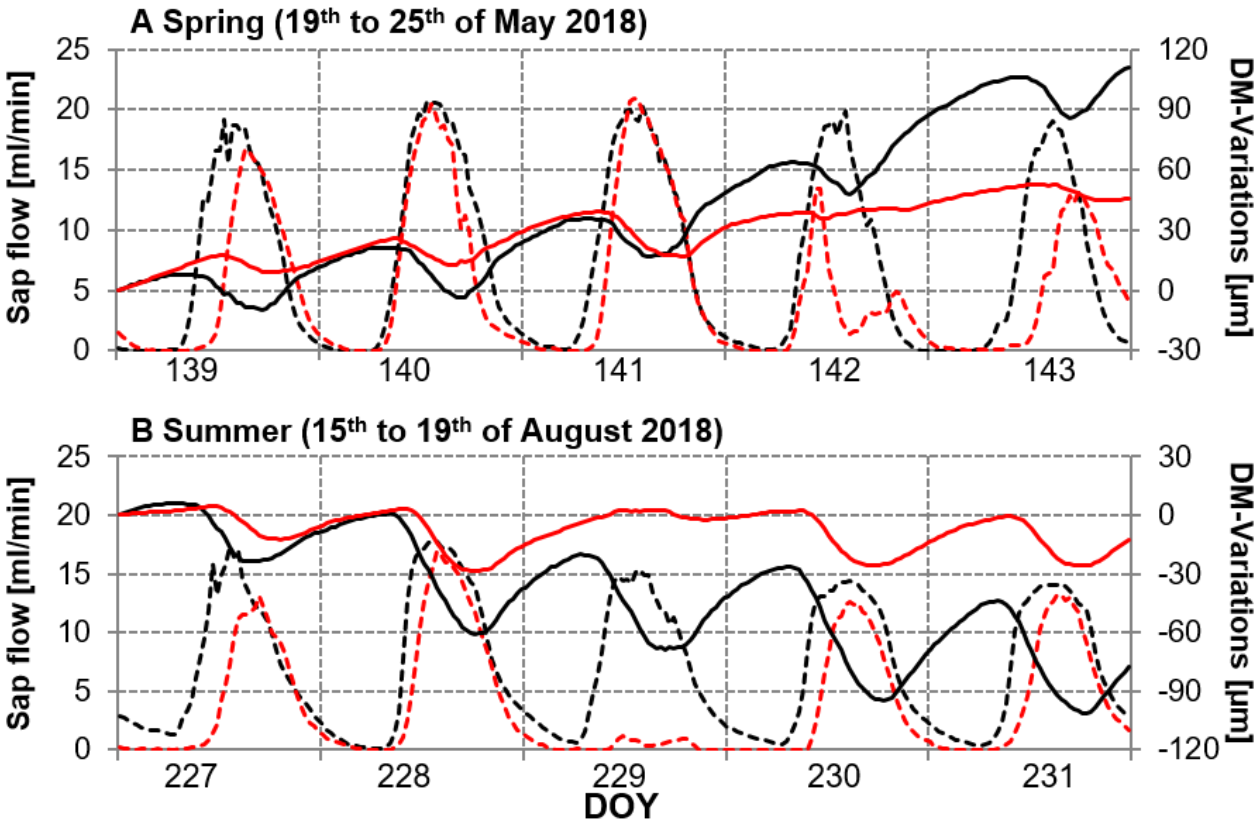

Figure 4. The mean diurnal cycles of the dendrometer (DM, solid lines) and sap flow (SF, dotted lines) data for both sites, EIF (red) and UWM (black) for 5 days in spring (**A**) and summer 2018 (**B**). For better illustration, the DM–data was set to zero on the first day of the example period.

3.4. Physiological Reactions of Trees in 2018

Figure 5 illustrates the correlation of the daily climate data and the tree physiological parameters stem radial increment (DM–SRI) and daily sap flow (SF–SUM) by research site and synoptic conditions. The subdivision into wet/dry days in spring/summer 2018 revealed group sizes of 8 to 15 days per data category, which indicates that the critical values of significance differed from correlogram to correlogram. Therefore, the significant correlations in Figure 5 are marked by different colored bars. On wet days in spring (Figure 5A), the stem increment (DM–SRI) of both EIF spruce and UWM oaks was mainly controlled by the vapor pressure deficit (VPD). Spruce growth was also supported by rising temperatures (TMP) and radiation (RAD). On dry spring days, in contrast, only the spruce trees showed positive correlations between the stem growth and the climate parameters. For the oaks at the UWM site, no significant relation between stem growth and climate was observed.

In summer 2018, the climate to growth feedback was completely different from that in spring. On wet days, only spruce showed a significant correlation between the stem growth and climate data—however not with the VPD, TMP, or RAD, as in spring, but with the water supply (PCP). On dry summer days, in contrast, only the stem growth of the oaks showed a weak significant correlation with the average daily radiation (RAD_{ave}). Other significant correlations were not observed. The sap flow activity of spruce and oak strongly differed by species and season. In spring, the spruces showed strong to very strong positive correlations between the daily sap flow (SF–SUM) and all climate parameters except for precipitation (Figure 5A). Particularly high correlations were observed for the mean vapor pressure deficit (VPD_{ave}) and radiation.

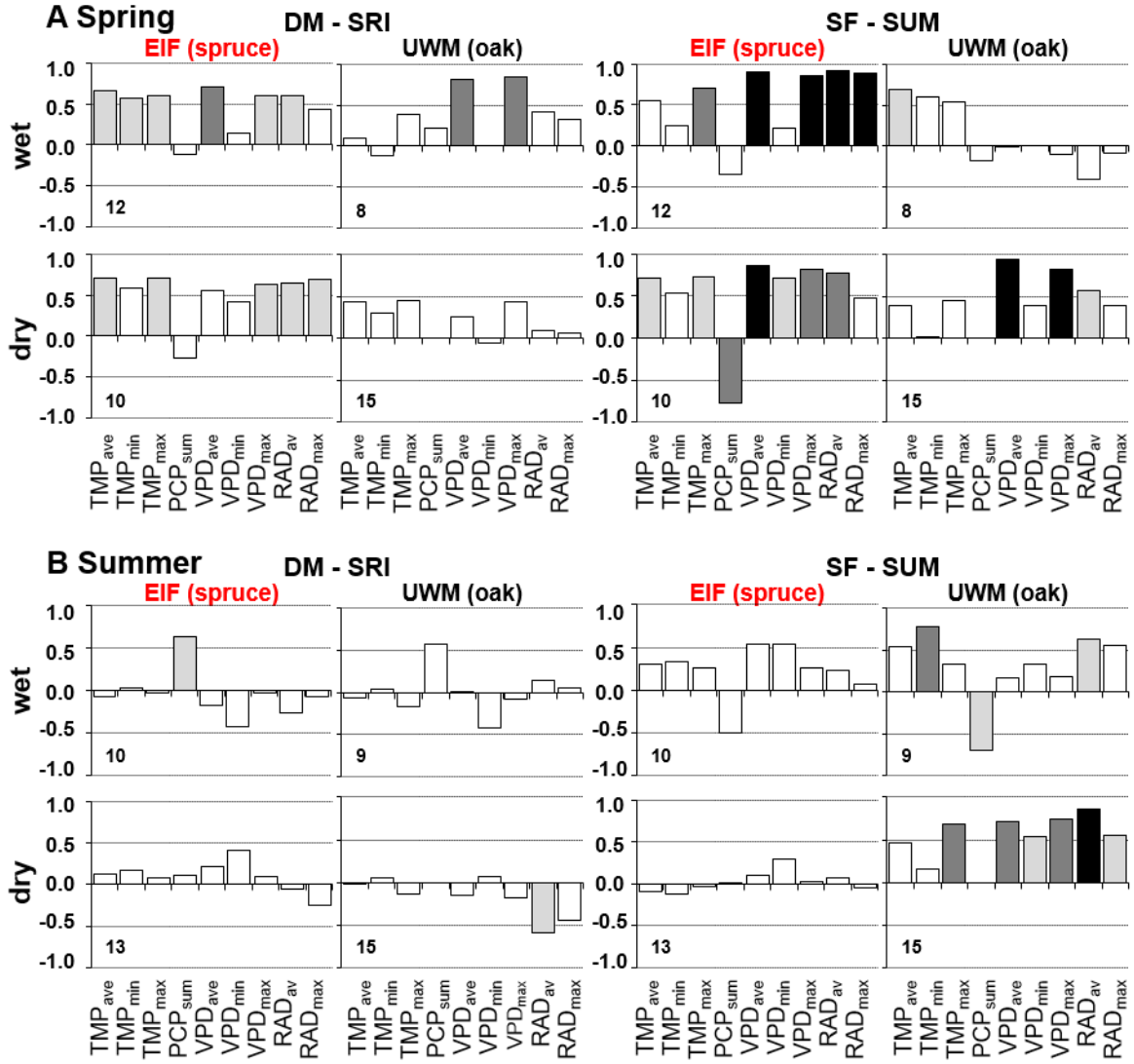

Figure 5. Pearson's correlations between the two tree type physiological parameters (stem radial increment DM–SRI), daily sum of sap flow (SF–SUM), and daily climate data by research site (EIF/UWM), and synoptic conditions (wet days/dry days) in (**A**) spring and (**B**) summer 2018. Wet days are defined as days with more than 3 mm rainfall, dry days as days with a precipitation sum of less than 3 mm for the actual day and the three days before. Bar colors illustrate levels of significance: black for a = 99.9%, dark grey for a = 99%, and light grey for a = 95%. The digits in the bottom left corner of each correlogram indicate the number of days falling in the analyzed data group. Abbreviations for the climate parameters from left to right: TMP_{ave} = mean daily temperature; TMP_{min} = daily minimum temperature; TMP_{max} = daily maximum temperature; PCP_{sum} = daily rainfall sum; VPD_{ave} = mean daily vapor pressure deficit; VPD_{min} = daily minimum of vapor pressure deficit; VPD_{max} = daily maximum of vapor pressure deficit; RAD_{ave} = mean daily solar radiation; and RAD_{max} = daily maximum of solar radiation. At the UWM site, no precipitation was detected on the dry spring and summer days. Therefore, correlations of the tree physiological parameters and precipitation sums were not calculated for this category.

On dry days, these correlations were slightly attenuated, and accompanied by a strongly negative correlation of the SF–SUM and daily precipitation (PCP_{sum}). The oaks, in contrast, only showed weakly significant correlations of the SF–SUM and daily mean temperature (TMP_{ave}) on wet days. On dry days, the SF–SUM strongly correlated with the VPD, and a weak correlation with mean daily radiation (RAD_{ave}) was observed. In summer, no significant correlations of the sap flow activity and climate parameters were found for spruce. The UWM oaks, in contrast, showed strong positive correlations of SF–SUM and the daily minimum temperature TMP_{min} on wet days, where weakly significant negative correlations with PCP were found. On dry days, all climate parameters except for PCP

showed positive correlations with SF–SUM. These correlations were particularly strong for the TMP_{max}, mean and maximum VPD, and RAD_{ave}.

4. Discussion

4.1. Climate/Growth Relationships

On both sites, the trees generally benefited from above–average precipitation and below–average temperatures during the growing season, with early summer precipitation being more important for the UWM–oaks and cooler temperatures being more important for the EIF–spruces (Figure 3). The positive growth responses of the EIF–spruces to generally cool conditions and a humid spring (Figure 3A) correspond well with other spruce studies in the German low mountain ranges [35,44,57,58], in the Black Forest [59] and in the lowlands of France [60] and Switzerland [61]. Only at higher altitudes above 1000 to 2000 m a.s.l., the negative temperature signal of spruce typically turns into a positive one [62–64].

With increasing continentality, the precipitation signal of spruce trees generally shifts from spring towards summer [65–67]. Hence, the EIF spruces with their spring precipitation signal clearly represent a maritime type of climate–growth relations. The climate signals of the UWM–oaks (Figure 3B), in contrast, differ from those typically found in the Eifel mountains [58,68] and others sites in northern and western Europe [69–72]. They strongly correspond to climate/growth signals as typically found for oaks in eastern and southeastern Europe [64,73–75]. With that, we assigned the UWM site with its negative summer temperature signal to a more continental growth type, for which different genetic characteristics of the sessile oaks could be responsible [76].

Despite this difference in site conditions and despite the differing ecological requirements of spruce and oak [77], two-thirds of the strong/extreme negative pointer years (PYs) coincide in both sites. While they can be explained by cold summers in 1965, 1973, and 1980, the causes of the growth decreases in the other six PYs (1976, 1991, 1995, 2000, 2006, and 2011) are due to heat waves in spring and/or summer and are also found in other regions of Central Europe [60,78–81].

Despite the spatial distance between the two research sites, we observed similar radial growth dynamics and similar growth reactions to extreme weather conditions across tree species. We explain this phenomenon by the adaptation of the trees to their location as postulated by Schweingruber & Nogler [82]. Only in case of negative temperature anomalies, which may be related to the formation of cold–air sinks, for example, did the general growth reaction become a bit more species specific. This is particularly valid for the year 1988, where we observed completely opposite growth reactions between EIF spruce and UWM oak: In both regions, the climate during the 1988 growing season was characterized by almost average weather conditions and exceptionally cold conditions in the growing season of the year before. For spruce, whose main distribution area is the European mountain zone [77], the low temperatures in 1987 did not cause any problems–in fact, rather the opposite, expressed by the observed above–average radial growth on the EIF site. Sessile oak, in contrast, is considered a warmth–loving species [83]. Hence, the cold summer months of 1987 disrupted growth so strongly that no carbohydrate reserves could be established in 1987, which would have been necessary to produce the first xylem cells in the following year 1988 [84]. The weather conditions in 1988, which were actually also favourable for sessile oak, could not prevent the strong growth depression resulting from the low temperature conditions of the previous year.

4.2. Specific Responses in 2018

In 2018, the trees at the two research sites showed opposite growth reactions: Due to the hot and dry summer, the EIF–spruces have developed a negative PY. The UWM–oaks, in contrast, showed above average wide tree rings (red bars in Figure 2C), which is surprising and does not correspond to the other findings on the climate–growth response of oaks during the European heat wave of 2018. In the North German Lowlands, for example,

Heinrich et al. [85] found significant growth reductions for oaks as a result of the early termination of the vegetation period.

In spring 2018, the physiological reaction of spruce and oak was still inconspicuous. Both species showed typical diurnal sap flow patterns, which essentially followed the VPD and radiation (Figures 4A and 5A). The dendrometers showed the respective inverse pattern of diurnal stem swelling and shrinking and an increasing daily maximum as a result of radial stem growth during the early growing season (Figure 4A). During the hot and dry summer of 2018, however, the physiological reaction of the trees completely changed (Figure 5B).

The spruces reacted as to be expected. As a response to heat and drought, they closed their stomata [14,16], which decoupled the sap flow activity and, respectively, the dendrometer curve, from the VPD and radiation: the DM–SRI and SF–SUM do not correlate with most of the climate parameters at this point. Only on wet days, a positive correlation between PCP and DM–SRI was observed and explained by the interim recovery of the stem water storage during and shortly after the precipitation event [16,84]. As a result of the stomatal closure during the day, the daily SF maxima in the summer were more than one quarter lower than those we observed in the spring. They decreased with the increasing duration of the dry period (Figure 4B). As a result of the persisting drought, the daily maxima of the dendrometer curve remained on a constant level and did no longer increase from day to day, which indicates that the radial growth was interrupted. The dendrometer still showed the typical diurnal variation, which inversely followed the reduced sap flow activity of the spruce. The interruption of cambial activity as indicated by the dendrometer data explains the formation of the negative PY for spruce (Figure 2C).

Like that of the EIF–spruces, the dendrometer data of the UWM–oaks hardly showed any correlation to the selected climate parameters in summer. Only on dry summer days, we observed a negative correlation of the DM–SRI and RAD indicating radial stem growth with reduced radiation input. The sap flow data of the UWM site, in contrast, strongly correlates with the climate data. Particularly on hot and dry summer days, where the spruces' sap flow activity was already completely decoupled from the climate data (Figure 5B), the sap flow of the UWM–oaks still increased with the increasing TMP_{max}, VPD, and RAD. Hence, the hydraulic system of the oaks was almost fully maintained even—or especially—in times of intensive solar radiation and despite the continuously declining soil water reserves.

At the same time, the daily maxima of the stem radii (dotted black line in Figure 4B) and, thus, the stem water reserves, decreased from day to day. This finding is in line with Dietrich et al. [86], who also found shrinking stem radii, but ongoing photosynthetic activity during the dry season of 2015 for sessile oaks near Basel, Switzerland. The authors explain this phenomenon with the ability of oaks to adapt their cell activity to the prevailing stem water potential: during phases of low water potential, for example, cell division may still take place; however, cell elongation and contraction can be reduced or even stopped due to the restricted water uptake from the soil. Instead, the trees covered their water demand almost entirely from the stem water storage. Applied to our setting, this means that due to the intensive use of the trunk's internal water resources, the oaks were able to maintain their hydraulic system, continue photosynthesis, produce carbohydrates, and form new cells. This allowed for the observed unexpected growth and the above–average tree–ring width despite the 2018 heat and drought (red bar in Figure 2C).

With that, the physiological response of the UWM–oaks to the extreme heat and drought in 2018 was completely different from that of the EIF–spruces. For the oaks, this appears to be a vital strategy for survival – they need to continue photosynthesis despite the heat and the associated evaporation losses, because they need to store nutrient and carbon reserves to initiate cell growth in the following year [87]. In contrast to the coniferous spruce, oaks cannot fall back on the needles of previous years to cover their nutrient demand in spring. As more than 95% of the water transport in oaks takes place in

the xylem cells of the current annual tree ring [14,88], they need to maintain photosynthesis and the related cell growth to survive.

5. Conclusions

In this study, we compared the responses of spruce and oak trees to the extreme environmental conditions during the European heat wave of 2018. Although the general long–term climate–growth relations of the analyzed forest stands were similar, the short–term physiological responses of the two tree species to the extreme heat and drought in 2018 were completely different. The coniferous spruce trees locked down their hydraulic systems and photosynthesis to prevent from excessive water loss and cavitation under drought.

This strategy resulted in a narrow tree ring and the formation of a negative pointer year. The oaks, in contrast, maintained water transport and photosynthesis to allow for continuing cell growth and covered their respective water demand essentially from the trees' internal stem water reserves. As a consequence, the oaks developed an above–average tree–ring width despite the extreme temperature and drought conditions. The extent to which the excessive use of stem water reserves is a sustainable strategy and when this strategy becomes harmful to the tree can only be clarified by follow–up investigations in subsequent years.

Supplementary Materials: The following are available online at https://www.mdpi.com/1999-4907/12/3/283/s1, Figure S1: Mean dendrometer data (lines) for UWM (black) and EIF (red) and corresponding ranges (colored areas) of three tress from 4th of April (DOY 100) to 15th of September (DOY 258), Figure S2: Mean plot of the sap flow densities (black lines) from 4 April to 15 September 2018 (DOY 100–258) and the associated range of measurements from the three individual trees for the UWM–oaks (A) and the EIF–spruces (B), Figure S3: Mean plot of sap flow densities (red lines) from 4 April to 15 September 2018 (DOY 100–258) and the associated range of measurements from the three individual trees for the EIF–spruces.

Author Contributions: B.N. conceived the ideas, processed the dendrometer data, performed data analysis, and wrote the paper. I.R. processed the sap flow data, contributed in the data collection, data analysis, and paper writing. J.B. contributed to the conceptual framework and paper writing. H.R.B. contributed and pre–processed data for the EIF site and contributed to the discussion of the results. B.T. contributed and pre–processed data for the UWM site and contributed to the discussion of the results. All authors have read and agreed to the published version of the manuscript.

Funding: The research in the Wüstebach Catchment in the Nationalpark Eifel was supported by TERENO (Terrestrial Environmental Observatories, funded by the Helmholtz–Gemeinschaft). The research in the Marburg Open Forest was funded by the Hessen State Ministry for Higher Education, Research and the Arts, Germany, as part of the LOEWE priority project Nature 4.0—Sensing Biodiversity, subproject UM2.

Data Availability Statement: Inquiries about data and research collaborations can be directed to the lead author (delawi@t-online.de). Data from the instrumentation in the Wüstebach catchment are freely available for download through the TERENO data portal (http://teodoor.icg.kfa-juelich.de/, access date: 12 February 2019). Data from the instrumentation in the Universitätswald Marburg are freely available for download through the LCRS data portal (http://www.lcrs.de/data_pre.do?citid=301, access date: 8 January 2019). Data from the DWD stations Kall-Sistig (station number 02497) and Gießen-Wettenberg (station number 01639) are freely available for download through the DWD Climate Data Center (https://opendata.dwd.de/climate_environment/CDC/observations_germany/climate/monthly/kl/, access date: 6 February 2019).

Acknowledgments: We thank the DWD (Deutscher Wetterdienst, German Meteorological Service) for providing weather data; thanks to A. Graf (FZ Jülich) and C. Drüe (FB Umweltmeteorologie, Uni Trier) for providing and processing the EIF EC–tower data. Finally, we thank M. Röös (Nationalpark Eifel) and A. Reinl (Marburg Open Forest, Revier Lahntal) for their cooperation and the necessary research permits.

Conflicts of Interest: The authors declare no conflict of interest.

References

1. Imbery, F.; Friedrich, K.; Koppe, C.; Janssen, W.; Pfeifroth, U.; Daßler, J.; Bissolli, P. *2018 Wärmster Sommer im Norden und Osten Deutschlands*; German Weather Service (DWD): Offenbach a. Main, Germany, 2018; p. 7.
2. Drouard, M.; Kornhuber, K.; Woollings, T. Disentangling Dynamic Contributions to Summer 2018 Anomalous Weather Over Europe. *Geophys. Res. Lett.* **2019**, *46*, 12537–12546. [CrossRef]
3. Pfleiderer, P.; Schleussner, C.-F.; Kornhuber, K.; Coumou, D. Summer weather becomes more persistent in a 2 °C world. *Nat. Clim. Chang.* **2019**, *9*, 666–671. [CrossRef]
4. Kornhuber, K.; Osprey, S.; Coumou, D.; Petri, S.; Petoukhov, V.; Rahmstorf, S.; Gray, L. Extreme weather events in early summer 2018 connected by a recurrent hemispheric wave-7 pattern. *Environ. Res. Lett.* **2019**, *14*, 054002. [CrossRef]
5. Kornhuber, K.; Coumou, D.; Vogel, E.; Lesk, C.; Donges, J.F.; Lehmann, J.; Horton, R.M. Amplified Rossby waves enhance risk of concurrent heatwaves in major breadbasket regions. *Nat. Clim. Chang.* **2019**, *10*, 48–53. [CrossRef]
6. Albergel, C.; Dutra, E.; Bonan, B.; Zheng, Y.; Munier, S.; Balsamo, G.; de Rosnay, P.; Muñoz–Sabater, J.; Calvet, J.C. Monitoring and forecasting the impact of the 2018 summer heatwave on vegetation. *Remote Sens.* **2019**, *11*, 520. [CrossRef]
7. Buras, A.; Rammig, A.; Zang, C.S. Quantifying impacts of the drought 2018 on European ecosystems in comparison to 2003. *Biogeosci. Discuss.* **2019**, *17*, 1655–1672. [CrossRef]
8. Maes, S.L.; Perring, M.P.; Vanhellemont, M.; Depauw, L.; Bulcke, J.V.D.; Brūmelis, G.; Brunet, J.; Decocq, G.; Ouden, J.D.; Härdtle, W.; et al. Environmental drivers interactively affect individual tree growth across temperate European forests. *Glob. Chang. Biol.* **2019**, *25*, 201–217. [CrossRef]
9. Vitasse, Y.; Bottero, A.; Cailleret, M.; Bigler, C.; Fonti, P.; Gessler, A.; Lévesque, M.; Rohner, B.; Weber, P.; Rigling, A.; et al. Contrasting resistance and resilience to extreme drought and late spring frost in five major European tree species. *Glob. Chang. Biol.* **2019**, *25*, 3781–3792. [CrossRef]
10. Vanhellemont, M.; Sousa-Silva, R.; Maes, S.L.; Bulcke, J.V.D.; Hertzog, L.; De Groote, S.R.; Van Acker, J.; Bonte, D.; Martel, A.; Lens, L.; et al. Distinct growth responses to drought for oak and beech in temperate mixed forests. *Sci. Total Environ.* **2019**, *650*, 3017–3026. [CrossRef]
11. Teskey, R.; Wertin, T.; Bauweraerts, I.; Ameye, M.; McGuire, M.A.; Steppe, K. Responses of tree species to heat waves and extreme heat events. *Plant Cell Environ.* **2015**, *38*, 1699–1712. [CrossRef] [PubMed]
12. Cook, E.R.; Seager, R.; Kushnir, Y.; Briffa, K.R.; Büntgen, U.; Frank, D.; Krusic, P.J.; Tegel, W.; Van Der Schrier, G.; Andreu-Hayles, L.; et al. Old World megadroughts and pluvials during the Common Era. *Sci. Adv.* **2015**, *1*, e1500561. [CrossRef]
13. Glaser, R.; Kahle, M. Reconstructions of droughts in Germany since 1500—Combining hermeneutic information and in-strumental records in historical and modern perspectives. *Clim. Past.* **2020**, *16*, 1207–1222. [CrossRef]
14. Hinckley, T.M.; Dougherty, P.M.; Lassoie, J.P.; Roberts, J.E.; Teskey, R.O. A Severe Drought: Impact on Tree Growth, Phenology, Net Photosynthetic Rate and Water Relations. *Am. Midl. Nat.* **1979**, *102*, 307. [CrossRef]
15. Levitt, J. *Responses of Plants to Environmental Stresses*; Academic Press: New York, NY, USA, 1972; 697p.
16. Zweifel, R.; Zimmermann, L.; Zeugin, F.; Newbery, D.M. Intra-annual radial growth and water relations of trees: Implications towards a growth mechanism. *J. Exp. Bot.* **2006**, *57*, 1445–1459. [CrossRef] [PubMed]
17. Hsiao, T.C.; Acevedo, E. Plant responses to water deficits, water-use efficiency, and drought resistance. *Agric. Meteorol.* **1974**, *14*, 59–84. [CrossRef]
18. Steppe, K.; De Pauw, D.J.W.; LeMeur, R.; Vanrolleghem, P.A. A mathematical model linking tree sap flow dynamics to daily stem diameter fluctuations and radial stem growth. *Tree Physiol.* **2006**, *26*, 257–273. [CrossRef] [PubMed]
19. Cook, B.I.; Wolkovich, E.M.; Parmesan, C. Divergent responses to spring and winter warming drive community level flowering trends. *Proc. Natl. Acad. Sci. USA* **2012**, *109*, 9000–9005. [CrossRef]
20. Haeni, M.; Zweifel, R.; Eugster, W.; Gessler, A.; Zielis, S.; Bernhofer, C.; Carrara, A.; Grünwald, T.; Havránková, K.; Heinesch, B.; et al. Winter respiratory C losses provide explanatory power for net ecosystem productivity. *J. Geophys. Res. Biogeosci.* **2016**, *122*, 243–260. [CrossRef]
21. Anderegg, W.R.L.; Schwalm, C.R.; Biondi, F.; Camarero, J.J.; Koch, G.W.; Litvak, M.; Ogle, K.; Shaw, J.D.; Shevliakova, E.; Williams, A.; et al. Pervasive drought legacies in forest ecosystems and their implications for carbon cycle models. *Science* **2015**, *349*, 528–532. [CrossRef] [PubMed]
22. Shao, J.; Zhou, X.; Luo, Y.; Li, B.; Aurela, M.; Billesbach, D.; Blanken, P.D.; Bracho, R.; Chen, J.; Fischer, M.; et al. Direct and indirect effects of climatic variations on the interannual variability in net ecosystem exchange across terrestrial ecosystems. *Tellus B Chem. Phys. Meteorol.* **2016**, *68*, 30575. [CrossRef]
23. Van Der Maaten-Theunissen, M.; Bümmerstede, H.; Iwanowski, J.; Scharnweber, T.; Wilmking, M.; Van Der Maaten, E. Drought sensitivity of beech on a shallow chalk soil in northeastern Germany—A comparative study. *For. Ecosyst.* **2016**, *3*, 24. [CrossRef]
24. Zweifel, R.; Sterck, F. A Conceptual Tree Model Explaining Legacy Effects on Stem Growth. *Front. For. Glob. Chang.* **2018**, *1*, 9. [CrossRef]
25. Leuzinger, S.; Zotz, G.; Asshoff, R.; Körner, C. Responses of deciduous forest trees to severe drought in Central Europe. *Tree Physiol.* **2005**, *25*, 641–650. [CrossRef]
26. Zweifel, R.; Eugster, W.; Etzold, S.; Dobbertin, M.; Buchmann, N.; Hasler, R. Link between continuous stem radius changes and net ecosystem productivity of a subalpine Norway spruce forest in the Swiss Alps. *New Phytol.* **2010**, *187*, 819–830. [CrossRef] [PubMed]

27. Weemstra, M.; Eilmann, B.; Sass-Klaassen, U.G.; Sterck, F.J. Summer droughts limit tree growth across 10 temperate species on a productive forest site. *For. Ecol. Manag.* **2013**, *306*, 142–149. [CrossRef]
28. Perkins, D.; Uhl, E.; Biber, P.; Du Toit, B.; Carraro, V.; Rötzer, T.; Pretzsch, H. Impact of Climate Trends and Drought Events on the Growth of Oaks (Quercus robur L. and Quercus petraea (Matt.) Liebl.) within and beyond Their Natural Range. *Forests* **2018**, *9*, 108. [CrossRef]
29. Harvey, J.E.; Smiljanić, M.; Scharnweber, T.; Buras, A.; Cedro, A.; Cruz-García, R.; Drobyshev, I.; Janecka, K.; Jansons, Ā.; Kaczka, R.; et al. Tree growth influenced by warming winter climate and summer moisture availability in northern temperate forests. *Glob. Chang. Biol.* **2020**, *26*, 2505–2518. [CrossRef] [PubMed]
30. Burri, S.; Haeler, E.; Eugster, W.; Haeni, M.; Etzold, S.; Walthert, L.; Braun, S.; Zweifel, R. How did Swiss forest trees respond to the hot summer 2015? *Die Erde* **2019**, *150*, 214–229.
31. Bogena, H.R.; Bol, R.; Borchard, N.; Brüggemann, N.; Diekkrüger, B.; Drüe, C.; Groh, J.; Gottselig, N.; Huismann, J.A.; Lücke, A.; et al. A terrestrial observatory approach to the integrated investigation of the effects of deforestration on water, energy, and matter fluxes. *Sci. China Earth Sci.* **2015**, *58*, 61–75.
32. Friess, N.; Bendix, J.; Brändle, M.; Brandl, R.; Dahlke, S.; Farwig, N.; Freisleben, B.; Holzmann, H.; Meyer, H.; Müller, T.; et al. Introducing Nature 4.0: A sensor network for environmental monitoring in the Marburg Open Forest. *Biodivers. Inf. Sci. Stand.* **2019**, *3*, 36389. [CrossRef]
33. Gottselig, N.; Wiekenkamp, I.; Weihermüller, L.; Brüggemann, N.; Berns, A.E.; Bogena, H.R.; Borchard, N.; Klumpp, E.; Lücke, A.; Missong, A.; et al. A three–dimensional view on soil biogeochemistry: A dataset for a forested headwater catchment. *J. Environ. Qual.* **2017**, *46*, 210–218. [CrossRef]
34. Hessen–Forst. *Forstbetriebsbuch*; 2017. FE_RPT_000-1.1.2; Stand: Kassel, Germany, 2017; Not Published.
35. Thomas, F.M.; Rzepecki, A.; Lücke, A.; Wiekenkamp, I.; Rabbel, I.; Pütz, T.; Neuwirth, B. Growth and wood isotopic signature of Norway spruce (Picea abies) along a small-scale gradient of soil moisture. *Tree Physiol.* **2018**, *38*, 1855–1870. [CrossRef]
36. Hurrell, J.W.; Kushnir, Y.; Ottersen, G.; Visbeck, M. An overview of the North Atlantic Oscillation. Climatic significance and environmental impact. *Geophys. Monogr.* **2003**, *134*, 1–35. [CrossRef]
37. Rabbel, I.; Bogena, H.; Neuwirth, B.; Diekkrüger, B. Using Sap Flow Data to Parameterize the Feddes Water Stress Model for Norway Spruce. *Water* **2018**, *10*, 279. [CrossRef]
38. Speer, J.H. *Fundamentals of Tree–Ring Research*; The University of Arizona Press: Tucson, AL, USA, 2018; 333p.
39. Rinn, F. TSAP–Win. In *Time Series Analysis and Presentation for Dendrochronology and Related Applications, Version 0.53 for Microsoft Windows*; User Reference: Heidelberg, Germany, 2003.
40. Stokes, M.A.; Smiley, T.L. *An Introduction to Tree–Ring Dating*; University of Arizona Press: Tucson, AL, USA, 1968; 73p, University of Chicago: Chicago, IL, USA, 1996.
41. Pilcher, J.R. Sample preparation, cross–dating and measurement. In *Methods of Dendrochronology*; Applications in the Environmental Sciences; Cook, E.R., Kairiukstis, L.A., Eds.; Kluwer Academic Publishers: Dordrecht, The Netherlands, 1990; pp. 40–51.
42. Cropper, J.P. Tree-Ring skeleton plotting by computer. *Tree Ring Bull.* **1979**, *39*, 47–59.
43. Neuwirth, B.; Esper, J.; Schweingruber, F.H.; Winiger, M. Site ecological differences to the climatic forcing of spruce pointer years from the Lötschental, Switzerland. *Dendrochronologia* **2004**, *21*, 69–78. [CrossRef]
44. Neuwirth, B.; Schweingruber, F.H.; Winiger, M. Spatial patterns of central European pointer years from 1901 to 1971. *Dendrochronologia* **2007**, *24*, 79–89. [CrossRef]
45. Jetschke, G.; van der Maaten, E.; van der Maaten–Theunissen, M. Towards the extremes: A critical analysis of pointer year detection methods. *Dendrochronologia* **2019**, *53*, 55–62. [CrossRef]
46. DesLauriers, A.; Anfodillo, T.; Rossi, S.; Carraro, V. Using simple causal modeling to understand how water and temperature affect daily stem radial variation in trees. *Tree Physiol.* **2007**, *27*, 1125–1136. [CrossRef]
47. DesLauriers, A.; Rossi, S.; Turcotte, A.; Morin, H.; Krause, C. A three-step procedure in SAS to analyze the time series from automatic dendrometers. *Dendrochronologia* **2011**, *29*, 151–161. [CrossRef]
48. Granier, A. Une nouvelle méthode pour la mesure du flux de sévebrute dans le tronc des arbres. *Ann. Sci. For.* **1985**, *42*, 193–200. [CrossRef]
49. Granier, A. Evaluation of transpiration in a Douglas-fir stand by means of sap flow measurements. *Tree Physiol.* **1987**, *3*, 309–320. [CrossRef]
50. Oishi, A.C.; Oren, R.; Stoy, P.C. Estimating components of forest evapotranspiration: A footprint approach for scaling sap flux measurements. *Agric. For. Meteorol.* **2008**, *148*, 1719–1732. [CrossRef]
51. Oishi, A.C.; Hawthorne, D.A.; Oren, R. Science Direct Baseliner: An open–source, interactive tool for processing sap flux data from thermal dissipation probes. *SoftwareX* **2016**, *5*, 139–143. [CrossRef]
52. Rabbel, I.; Diekkrüger, B.; Voigt, H.; Neuwirth, B. Comparing ΔTmax Determination Approaches for Granier-Based Sapflow Estimations. *Sensors* **2016**, *16*, 2042. [CrossRef]
53. Graf, A.; Bogena, H.R.; Drüe, C.; Hardelauf, H.; Putz, T.; Heinemann, G.; Vereecken, H. Spatiotemporal relations between water budget components and soil water content in a forested tributary catchment. *Water Resour. Res.* **2014**, *50*, 4837–4857. [CrossRef]
54. Koubaa, A.; Isabel, N.; Zhang, S.Y.; Beaulieu, J.; Bousquet, J. Transition from juvenile to mature wood in black spruce (Picea mariana (Mill.) B.S.P.). *Wood Fiber Sci.* **2005**, *37*, 445–455.

55. Babst, F.; Carrer, M.; Poulter, B.; Urbinati, C.; Neuwirth, B.; Frank, D. 500 years of regional forest growth variability and links to climatic extreme events in Europe. *Environ. Res. Lett.* **2012**, *7*, 045705. [CrossRef]
56. Russo, S.; Sillmann, J.; Fischer, E.M. Top ten European heatwaves since 1950 and their occurrence in the coming decades. *Environ. Res. Lett.* **2015**, *10*, 124003. [CrossRef]
57. Friedrichs, D.A.; Trouet, V.; Büntgen, U.; Frank, D.C.; Esper, J.; Neuwirth, B.; Löffler, J. Species-specific climate sensitivity of tree growth in Central-West Germany. *Trees* **2009**, *23*, 729–739. [CrossRef]
58. Fischer, S.; Neuwirth, B. Klimasensitivität der Douglasie in Eifel und Kellerwald [Climate sensitivityof Douglas–fir in Eifel and Kellerwald]. *Allg. Forst Jagdztg.* **2012**, *183*, 23–32.
59. Van der Maaten–Theunissen, M.; Kahle, H.P.; van der Maaten, E. Drought sensitivity of Norway spruce is higher than that of silver fir along an altitudinal gradient in southwestern Germany. *Ann. For. Sci.* **2013**, *70*, 185–193. [CrossRef]
60. Lebourgeois, C.; Rathgeber, B.K.; Ulrich, E. Sensitivity of French temperate coniferous forests to climate variability and extreme events (Abies alba, Picea abies and Pinus sylvestris). *J. Veg. Sci.* **2010**, *21*, 364–376. [CrossRef]
61. Lévesque, M.; Rigling, A.; Bugmann, H.; Weber, P.; Brang, P. Growth response of five co-occurring conifers to drought across a wide climatic gradient in Central Europe. *Agric. For. Meteorol.* **2014**, *197*, 1–12. [CrossRef]
62. Büntgen, U.; Frank, D.C.; Schmidhalter, M.; Neuwirth, B.; Seifert, M.; Esper, J. Growth/climate response shift in a long subalpine spruce chronology. *Trees* **2005**, *20*, 99–110. [CrossRef]
63. Hartl-Meier, C.; Zang, C.; Dittmar, C.; Esper, J.; Göttlein, A.; Rothe, A. Vulnerability of Norway spruce to climate change in mountain forests of the European Alps. *Clim. Res.* **2014**, *60*, 119–132. [CrossRef]
64. Ponocná, T.; Spyt, B.; Kaczka, R.; Büntgen, U.; Treml, V. Growth trends and climate responses of Norway spruce along ele-vational gradients in East–Central Europe. *Trees* **2016**, *30*, 14. [CrossRef]
65. Rybníček, M.; Čermák, P.; Prokop, O.; Žid, T.; Trnka, M.; Kolář, T. Oak (*Quercus* spp.) response to climate differs more among sites than among species in central Czech Republic. *Dendrobiology* **2016**, *75*, 55–65. [CrossRef]
66. Kolář, T.; Čermák, P.; Trnka, M.; Žid, T.; Rybníček, M. Temporal changes in the climate sensitivity of Norway spruce and European beech along an elevation gradient in Central Europe. *Agric. For. Meteorol.* **2017**, *239*, 24–33. [CrossRef]
67. Čermák, P.; Kolář, T.; Žid, T.; Trnka, M.; Rybníček, M. Norway spruce responses to drought forcing in area affected by forest decline. *For. Syst.* **2019**, *28*, e016. [CrossRef]
68. Friedrichs, D.A.; Büntgen, U.; Frank, D.C.; Esper, J.; Neuwirth, B.; Löffler, J. Complex climate controls on 20th century oak growth in Central-West Germany. *Tree Physiol.* **2008**, *29*, 39–51. [CrossRef]
69. Drobyshev, I.; Niklasson, M.; Eggertsson, O.; Linderson, H.; Sonesson, K. Influence of annual weather on growth of pedunculate oak in southern Sweden. *Ann. For. Sci.* **2008**, *65*, 512. [CrossRef]
70. Härdtle, W.; Niemeyer, T.; Assmann, T.; Aulinger, A.; Fichtner, A.; Lang, A.; Leuschner, C.; Neuwirth, B.; Pfister, L.; Quante, M.; et al. Climate responses of tree–ring width and d13C signatures of sessile oak (Quercus petraea Liebl.) on soils with contrasting water supply. *Plant. Ecol.* **2013**, *214*, 1147–1156. [CrossRef]
71. Scharnweber, T.; Manthey, M.; Wilmking, M. Differential radial growth patterns between beech (*Fagus sylvatica* L.) and oak (Quercus robur L.) on periodically waterlogged soils. *Tree Physiol.* **2013**, *33*, 425–437. [CrossRef] [PubMed]
72. García-Suárez, A.; Butler, C.; Baillie, M. Climate signal in tree-ring chronologies in a temperate climate: A multi-species approach. *Dendrochronologia* **2009**, *27*, 183–198. [CrossRef]
73. Wazny, T.; Eckstein, D. Dendrochronological signal of oak (*Quercus* spp.) in Poland. *Dendrochronologia* **1991**, *9*, 181–191.
74. Bronisz, A.; Bijak, S.; Bronisz, K.; Zasada, M. Climate influence on radial increment of oak (*Quercus* spp.) in central Poland. *Geochronometria* **2012**, *39*, 276–284. [CrossRef]
75. Nechita, C.; Popa, I.; Eggertsson, Ó. Climate response of oak (*Quercus* spp.), an evidence of a bioclimatic boundary induced by the Carpathians. *Sci. Total Environ.* **2017**, *599*, 1598–1607. [CrossRef]
76. Torres-Ruiz, J.M.; Kremer, A.; Murphy, M.R.C.; Brodribb, T.; Lamarque, L.J.; Truffaut, L.; Bonne, F.; Ducousso, A.; Delzon, S. Genetic differentiation in functional traits among European sessile oak populations. *Tree Physiol.* **2019**, *39*, 1736–1749. [CrossRef] [PubMed]
77. Ellenberg, H.; Leuschner, C. *Vegetation Mitteleuropas mit den Alpen in Ökologischer, Dynamischer und Historischer Sicht*, 6th ed.; Ulmer Verlag: Stuttgart, Germany, 2010; 1357p.
78. Rybníček, M.; Čermák, P.; Kolář, T.; Žid, T. Growth responses of Norway spruce (*Picea abies* (L.) Karst.) to the climate in the south-eastern part of the Českomoravská Upland (Czech Republic). *Geochronometria* **2012**, *39*, 149–157. [CrossRef]
79. Fischer, S.; Neuwirth, B. Vulnerability of Trees to Climate Events in Temperate Forests of West Germany. *ISRN For.* **2013**, *2013*, 201360. [CrossRef]
80. Čejková, A.; Poláková, S. Growth responses of sessile oak to climate and hydrological regime in the Zbytka Nature Reserve, Czech Republic. *Geochronometria* **2012**, *39*, 285–294. [CrossRef]
81. Becker, M.; Nieminen, T.M.; Gérémia, F. Short–term variations and long–term changes in oak productivity in northeastern France. *Ann. Sci. For.* **1994**, *51*, 477–492. [CrossRef]
82. Schweingruber, F.H.; Nogler, P. Synopsis and climatological interpretation of Central European tree–ring sequences. *Bot. Helv.* **2003**, *113*, 125–143.
83. Larcher, W. *Physiological Plant Ecology*; Springer: Berlin, Germany, 1995; 513p.

84. Barbaroux, C.; Breda, N. Contrasting distribution and seasonal dynamics of carbohydrate reserves in stem wood of adult ring-porous sessile oak and diffuse-porous beech trees. *Tree Physiol.* **2002**, *22*, 1201–1210. [CrossRef]
85. Heinrich, I.; Balanzategui, D.; Bens, O.; Blume, T.; Brauer, A.; Dietze, E.; Gottschalk, P.; Güntner, A.; Harfenmeister, K.; Helle, G.; et al. System Erde. *GFZ J.* **2019**, *9*, 38–48. [CrossRef]
86. Dietrich, L.; Zweifel, R.; Kahmen, A. Daily stem diameter variations can predict the canopy water status of mature temperate trees. *Tree Physiol.* **2018**, *38*, 941–952. [CrossRef]
87. Hoch, G.; Richter, A.; Körner, C. Non-structural carbon compounds in temperate forest trees. *Plant Cell Environ.* **2003**, *26*, 1067–1081. [CrossRef]
88. Bréda, N.; Granier, A. Intra- and interannual variations of transpiration, leaf area index and radial growth of a sessile oak stand (Quercus petraea). *Ann. Sci. For.* **1996**, *53*, 521–536. [CrossRef]